Performance of Cross and Buttress Walls to Control Wall Deflection Induced by Deep Excavation in Dense Urban Area

A. Lim[1] and C. Y. Ou[2]
[1] *Department of Civil Engineering, Universitas Katolik Parahyangan, Bandung 40141, Indonesia.*
[2] Department of Civil and Construction Engineering, National Taiwan University of Science and Technology, Taipei 10607, Taiwan.
E-mail: aswinlim@unpar.ac.id

ABSTRACT: The paper presents the performance of two deep excavation Case-histories and their three-dimensional finite element analyses. Case 1 describes the application of cross walls and buttress walls in controlling the diaphragm wall deflection and avoiding the low-story adjacent buildings from damages, in which those low-story buildings were founded on shallow foundations and located 1 to 2 m from the excavated area. Moreover, Case 2 demonstrates the application of cross walls and buttress walls to limit the movement of adjacent existing twin metro tunnels induced by deep excavation. In addition, the diaphragm wall of Case 2 defected due to heavy rain while concreting process and causing the excavation more challenging to be executed safely. Three-dimensional finite element analyses were conducted to simulate and examine the performance of cross and buttress walls to control movements induced by deep excavation. The result shows that the cross walls have a significant effect in controlling deformations induced by deep excavation. The dense interval between cross walls could yield a very rigid retaining wall system and cause very small wall deflections. The measure can be used for an excavation project nearby metro systems to reduce the potential settlement of the metro tunnels.

KEYWORDS: Deep Excavation, Wall Deflection, Cross Wall, Buttress Wall, Three-dimensional Analysis

1. INTRODUCTION

Nowadays, deep excavations in dense urban areas are quite challenging because they should protect adjacent buildings or infrastructures, such as existing metro tunnels from damages caused by excessive movements induced by deep excavations. The problem becomes more severe when the soft soil is predominant in the area. Hence, anticipated auxiliary measures should be designed prior to excavation to maintain the stability and the integrity of adjacent properties.

Some of the widely used auxiliary measures are cross walls and buttress walls. Figure 1 illustrates the layout of cross walls and buttress walls. The buttress wall is a concrete wall perpendicular to the diaphragm wall constructed before excavation and it is not connected to the opposite diaphragm wall. If it is connected to the opposite diaphragm wall, then it is called the cross wall. The connection between cross/buttress walls and diaphragm walls should be rigid and watertight and form an integral body. The construction technique and equipment of cross walls and buttress walls are similar to the construction technique and equipment of diaphragm walls (Ou et al., 2006).

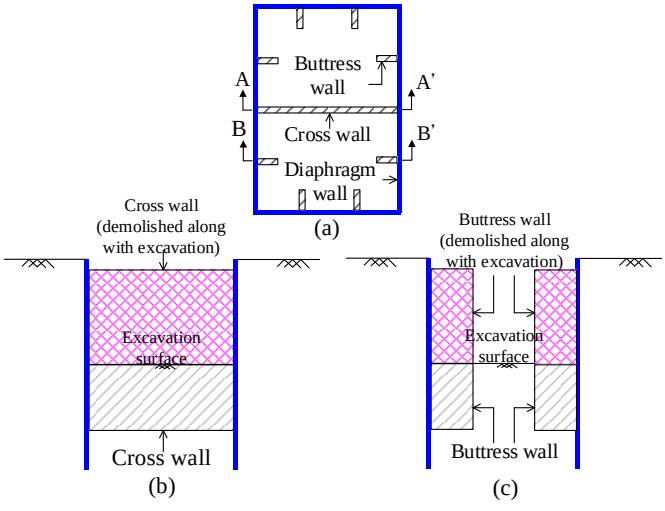

Figure 1 Schematic diagram of the cross wall and buttress wall (a) plan view, (b) section A-A', (c) section B-B'

The use of buttress walls and/or cross walls as an auxiliary measure to control movements induced by deep excavation is well-known in some Asia countries. Some successful excavation Case histories with the application of buttress wall solely, or combinations with the cross wall to control movements induced by deep excavation have been reported (Hsieh et al., 2013., Hsieh et al., 2015., Hwang and Moh, 2008., Lim et al., 2016., Ou et al., 2008., Ou et al., 2006., Ou et al., 2011). Those reported Case histories described the protection of adjacent buildings which were located near the ground surface.

In this paper, two new Case histories with the installation of cross walls and buttress walls are studied. The first Case describes the application of cross walls and buttress walls in controlling the diaphragm wall deflection and avoiding the low-story adjacent buildings from damages, in which those low-story buildings were founded on shallow foundations and located 1 to 2 m from the excavated area. Moreover, the second Case demonstrates the application of cross walls and buttress walls to limit the movement of adjacent existing twin metro tunnels induced by deep excavation, which was located 14.5 m from the excavated area and 13.7 m in depth. In addition, the diaphragm wall of the second Case has some defects due to heavy rain while concreting process and causing the excavation more challenging to be executed safely. Later, three-dimensional finite element analyses were conducted to simulate and examine the performance of cross and buttress walls to control movements induced by deep excavation.

2. THREE-DIMENSIONAL FINITE ELEMENT ANALYSIS

PLAXIS 3D v.2013 (Brinkgreve et al., 2013) was used to perform the three-dimensional finite element analysis. The Hardening Soil (HS) model (Schanz et al., 1999) was adopted to simulate the soil behavior, including the fine-grained soil and the coarse-grained soil under the undrained and drained conditions, respectively. Of the HS parameters; the secant stiffness (E_{50}^{ref}) corresponding to the reference stress, p^{ref}, the tangent referential stiffness for primary oedometer loading (E_{oed}^{ref}), the unloading/reloading referential stiffness (E_{ur}^{ref}), and the power for stress-level dependency of stiffness (m); were evaluated according to Lim and Ou (2017) and

Calvello and Finno (2004) for the clay, and to Khoiri and Ou (2013) for the coarse-grained soils under drained conditions.

In the analyses of fine-grained soil, an elastic unloading/reloading Young's modulus was mathematically derived based on a result of oedometer tests (Ou, 2016), as shown in Eq. (1), which e is void ratio, p' is mean effective stress, $\kappa = Cs/\ln 10$, where Cs is swelling index, and υ_{ur} is unloading-reloading Poisson's ratio of soil.

$$E_{ur} = \frac{3(1+e)p'(1-2\upsilon_{ur})}{\kappa} \quad (1)$$

In order to be used as an input parameter in the HS model, E_{ur} should be converted to the E_{ur}^{ref} as proposed by Schanz et al., (1999), as shown in Eq. (2).

$$E_{ur} = E_{ur}^{ref}\left(\frac{c.\cos\phi - \sigma_3'\sin\phi}{c.\cos\phi + p^{ref}\sin\phi}\right)^m \quad (2)$$

When E_{ur}^{ref} is determined, then $E_{50}^{ref} = 1/3E_{ur}^{ref}$ and $E_{oed}^{ref} = 0.7E_{50}^{ref}$ can be estimated as suggested by Calvello and Finno (2004). The coefficient of the at-rest earth pressure for the coarse-grained soil was calculated from Jaky (1944) which was $K_0 = 1-\sin\phi'$ and the coefficient of the at-rest earth pressure for the fine-grained soil was estimated based on Ladd et al., (1977) which was $K_{0,OC} = (1-\sin\phi')\mathrm{OCR}^{\sin\phi'}$.

The structural members, such as diaphragm walls, buttress walls, cross walls, tunnel lining and concrete floor slabs, were assumed to behave as the linear-elastic material. The stiffness of diaphragm walls was reduced by 20% from its nominal value, considering that the stiffness of the concrete diaphragm wall reduces when a large bending moment of the diaphragm wall causes the occurrence of cracks in the concrete (Lim et al., 2010). The soil stress redistribution might be generated due to the installation of diaphragm walls and buttress walls and its quality of construction, for example, continuous or discontinuous wall (Comodromos et al., 2013). But, the numerical analysis might not be able to model all of the installation effects precisely. For simplification, the diaphragm wall and buttress wall were assumed to be wished in place (Hsieh et al., 2013, Dong et al., 2016, Lim et al., 2016) with the consideration of the weight of the concrete from the diaphragm wall and buttress wall over the existing soil. The Poisson's ratio of concrete was assumed 0.2. In addition, the temporary struts and the concrete floor slabs were installed right after each stage of excavation. Both cross walls and buttress walls would be demolished along with excavation stages until the end of excavation.

According to ACI 318-95 (1995) code, the nominal value of concrete Young's modulus could be estimated by using an equation $E_c = 4700\sqrt{f_c'}$ (unit: MPa), where f_c' is the compressive strength of concrete (unit: MPa). In the analyses, the interface friction (R_{inter}) between the structural elements and adjacent soils was set as rigid (R_{inter}=1) and its behavior follows the Mohr-Coulomb model (Hsieh et al., 2013, Lim et al., 2016).

Ten-node tetrahedral elements were employed to simulate the soil volume, 6-node plate elements were used to model the diaphragm wall, the concrete slab, and the buttress wall. The node-to-node element was utilized to model the struts. Moreover, 12-node interface elements were applied to model the soil-plate element interaction behavior. Soil movements normal to the four vertical sides were restrained while they were restrained in all directions at the bottom of the geometry. In addition, the distance between the diaphragm wall and the outer boundary of mesh was ensured to be larger than two times of the final excavation depth to minimize the boundary effect.

Furthermore, all analyses were performed in full-scale and the significance adjacent structures were also modeled. In Case 1, all of the adjacent buildings were founded on shallow foundations. Thus, the adjacent buildings were simply modeled with a uniform loading acting on the plate element (Hsieh et al., 2015). It should be noted that the stiffness of adjacent building was neglected. According to Elshafie et al., (2013), modeling the stiffness of adjacent building would affect the profile of excavation-induced settlement. A stiff building behind the retaining wall tilted during excavation with very little curvature exhibited. As a consequence, the soil underneath, constrained by the building above, has no option but to follow the settlement profile of the building. A 15 kPa uniform loading was assumed to model one story of the buildings. Since those adjacent buildings were more than 10 years old, the excess pore water pressure induced by the loading of those buildings was assumed to fully dissipate. Hence, in modeling, the full dissipation of excess pore water pressure in undrained soil layers was conducted prior to excavation.

3. CASE STUDY 1

3.1 Project overview of Case 1

Case 1 is a new well-documented case history which was located in Taipei, Taiwan. The building is a 13-stories building with three levels of basement. Figure 2 shows the layout of the excavation along with the location of inclinometers and adjacent buildings. The adjacent buildings were dominated by two-story and three-story old buildings, and the closest distance to the excavation area is about 1 to 2 m only, which was located on the east and west diaphragm walls. The south side of the excavation area is a main road with 18

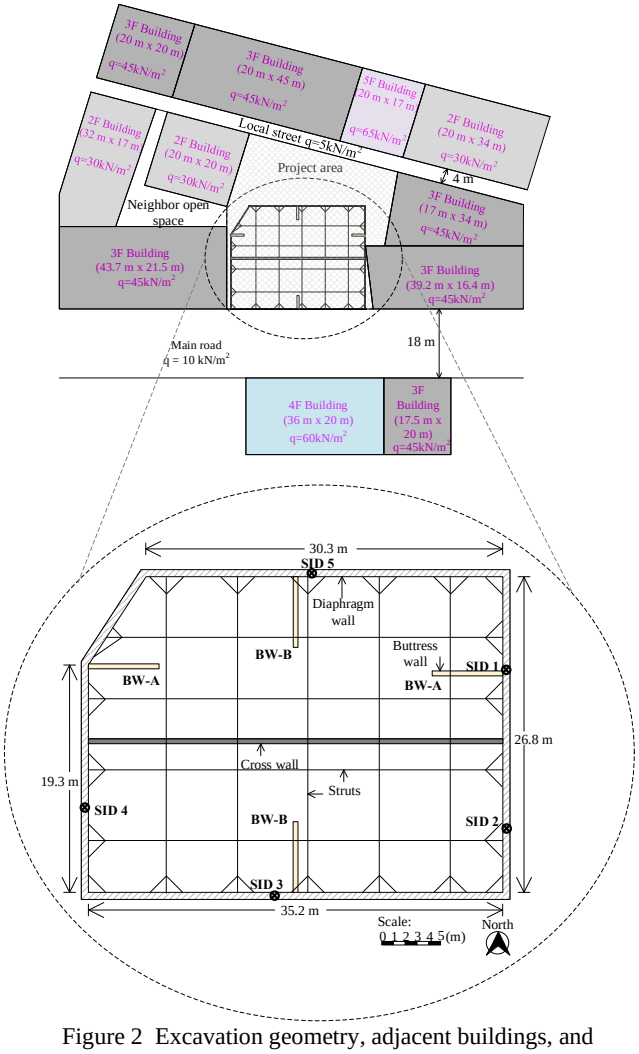

Figure 2 Excavation geometry, adjacent buildings, and instrumentation for Case 1

m in width, and the north side of the excavation area is a street with 4 m in width. Adjacent to the street, a block of low-story buildings also exists. In Case 1, the main concern is to protect the adjacent buildings which were located on the east and west side because the distance is very close. Thus, the 0.6 m thick cross wall was designed from GL -2 m to GL -23.5 m. In addition, the buttress walls type A (BW-A) with 6 m in length were also designed from GL -2 m to GL -14.9 m (height is 12.9 m). Then the buttress walls type B (BW-B) with 6 m in length and 21.5 in height were also constructed at the south and north walls to minimize the main road settlement induced by excavation.

The excavation depth was 11.9 m, which was completed using the bottom-up construction method a shown in Figure 3. As shown in Figure 3, the excavation was supported by 4 levels of struts. The thickness of diaphragm wall was 0.7 m and the depth of the wall was 26.5 m for the north and south walls and 28.5 m for the west and east walls. The unconfined compressive strength of concrete (f_c') used for the diaphragm wall and the bottom section of the cross and buttress walls (GL -11.9 m to GL-23.5 m) was 27.5 MPa. Meanwhile, a low strength concrete with f_c' =10.3 MPa was used for the upper section of the cross and buttress walls because the low strength concrete would be easier to be demolished.

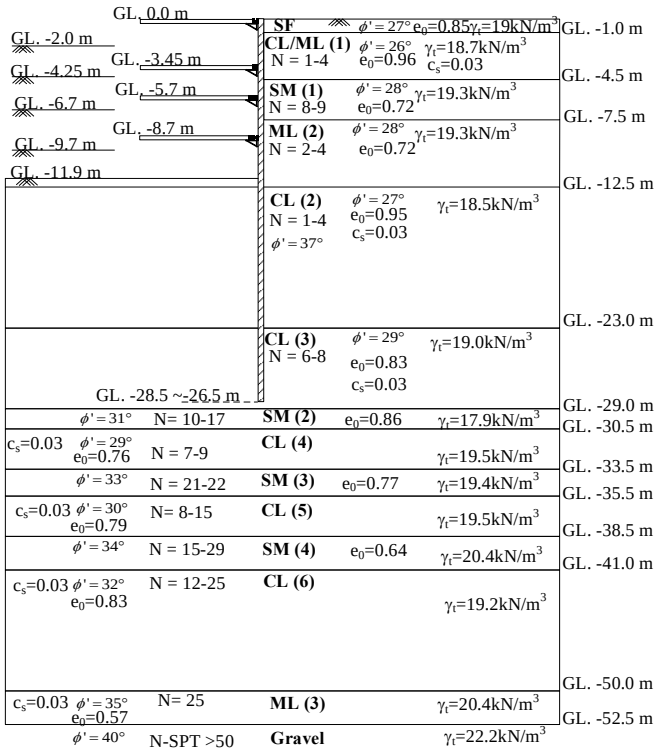

Figure 3 Profile of the excavation sequence and subsurface soil layers for Case 1

3.2 Subsurface soil profile and soil parameters of Case 1

Figure 3 shows the profile of the excavation and the subsurface soil conditions along with their physical properties and strength parameters which were obtained from the laboratory soil investigation. The groundwater level was located at GL -2.5 m. The excavation depth was 11.9 m, which was completed in six stages using the bottom-up construction method and the modeling stages were listed in Table 1. In brief, each level of struts was installed directly after an excavation stage. After stage 1, groundwater inside excavation zone was pumped out from SM(1) and ML(2) soil layers until GL -12.5 m. Initially, the ML(2) layer was not expected for dewatering because it was assumed to have low permeability. However, during the construction process, the groundwater inside the ML(2) layer could also be pumped out easily. It indicates that the permeability of the ML(2) layer is quite high. The purpose of dewatering in this project is to ease the soil excavation. Thus, the ML(2) of Case 1 was modeled as the drained material. In addition, both the cross wall and the buttress walls were demolished with excavation process.

Table 2 and Table 3 list the wall and struts parameters used for analysis, respectively. Furthermore, Table 4 lists the soil parameters used for analysis. All of the parameters in the tables were evaluated according to the methods discussed in the preceding section.

3.3 Finite element mesh of Case 1

Figure 4.(a) show the three-dimensional finite element mesh of Case 1. The boundaries in the horizontal directions (x- and y-directions) were placed at a distance of four times the excavation depth behind the wall to minimize the boundary effect, and the boundary in the depth direction (z-direction) was placed at the bedrock. The boundary of the bottom surface was restrained in all directions, and the vertical boundaries were restrained in the horizontal direction. The same boundaries also applied to Case 2. Moreover, Figures 4.(b) and (c) show the mesh of retaining wall system at initial condition and at a final condition, respectively. The structural members consisted of diaphragm walls, buttress walls and cross walls (modeled with the plate element) and struts (modeled with the node-to-node anchor).

Table 1 Simulation stages of excavation for Case 1

Stage	Activities
0	Initial condition
0-a	Activate adjacent buildings
0-b	Dissipate excess pore pressure
0-c	Install retaining system
0-d	Reset displacement to zero
0-e	Activate traffic loadings
1	Excavate -2.0 m
2	Dewatering the SM-1 and ML-2 to -12.5 m
3	Install struts level 1 + preloading 600 kN Excavate -4.25 m
4	Install struts level 2 + preloading 900 kN Excavate -6.7 m
5	Install struts level 3 + preloading 1200 kN Excavate -9.7 m
6	Install struts level 4 + preloading 1200 kN Excavate -11.9 m

Table 2 The walls input parameters for Case 1

Type	Model	t (m)	f_c' (MPa)	E (kPa)	γ (kN/m^3)
Diaphragm wall	Plate	0.7	27.45	24624591	24
Buttress and cross walls-up		0.6	10.3	15083998	24
Buttress and cross walls-down		0.6	27.45	24624591	24

Table 3 The struts input parameters for Case 1

Strut	Model	A (m^2)	E (GPa)	Component
Hx350x350x12x19	Node-to-node anchor	0.0174	210	1st and 2nd level-strut and 1st level-wale
Hx400x400x13x21		0.0219		2nd level-wale
2Hx350x350x12x19		0.0348		3rd level-strut and wale
2Hx400x400x13x21		0.0437		4th level strut and wale
H200x200x8x12		0.0064		1st and 2nd-corner and end braces
H250x250x9x14		0.0092		3rd and 4th-corner and end braces

3.4 Analysis result and discussion of Case 1

Although the analysis was performed in full-scale, only the wall deflection at SID-1, SID-2, and SID-4 was discussed because they were the main focus of the application of the cross wall and the buttress walls. Indeed, the ground settlement induced by excavation at the main road (south) and the street (north) was about 5 to 10 mm only and it was very small. Figure 5 shows the comparison of the field measurements and the computed lateral wall deflections for the Case 1.

Table 4 Soil input parameters for Case 1

Soil layer	Depth (m)	Description	Drainage type	γ_t (kN/m^3)	OCR	K_0	ϕ' (deg)	c' (kPa)	E_{50}^{ref} (kPa)	E_{oed}^{ref} (kPa)	E_{ur}^{ref} (kPa)	m
1	0 - 1	SF	Undrained	19.0	2.5	0.83	27	0	8164	5715	24491	1
2	1 -4.5	CL/ML (1)	Undrained	18.7	1.5	0.69	26	0	10391	7274	31174	1
3	4.5 - 7.5	SM (1)	Drained	19.3	1	0.53	28	0	11986	17979	35958	0.5
4	7.5 - 12.5	ML (2)	Drained	19.3	1	0.53	28	0	4973	7460	14920	0.5
5	12.5 - 23	CL (2)	Undrained	18.5	1	0.55	27	0	11469	8028	34407	1
6	23 - 29	CL (3)	Undrained	19.0	1	0.52	29	0	11071	7750	33213	1
7	29 - 30.5	SM (2)	Drained	17.9	1	0.48	31	0	11644	17465	34931	0.5
8	30.5 - 33.5	CL (4)	Undrained	19.5	1	0.52	29	0	10647	7453	31942	1
9	33.5 -35.5	SM (3)	Drained	19.4	1	0.46	33	0	16807	16807	50422	0.5
10	35.5 - 38.5	CL (5)	Undrained	19.5	1	0.50	30	0	10991	7694	32973	1
11	38.5 - 41	SM (4)	Drained	20.4	1	0.44	34	0	18194	18194	54583	0.5
12	41 - 50	CL (6)	Undrained	19.2	1	0.47	32	0	11594	8116	34783	1
13	50 - 52.5	ML (3)	Undrained	20.4	1	0.43	35	0	10472	7330	31415	1
14	52.5 - 65	Gravel	Undrained	22.2	1	0.36	40	0	85000	85000	255000	0.5

Note: p^{ref} = 100kPa and υ_{ur} = 0.2 for all types of soils

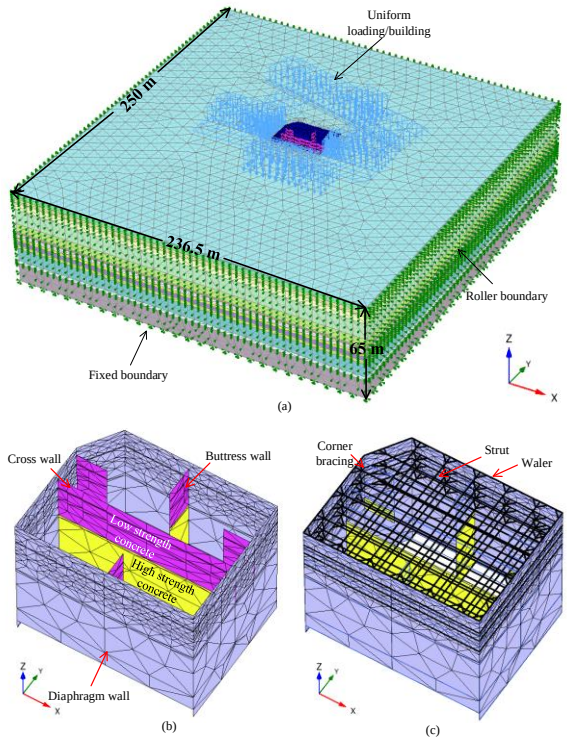

Figure 4 Three-dimension finite element mesh for Case 1 analysis (a). Overall mesh, (b) retaining wall mesh before excavation, (c) retaining wall mesh at the end of the excavation

It was supposed that the wall deflection at SID 1 could smaller than the wall deflection at SID 2 because the buttress wall type A (BW-A) was installed near the SID-1. But, the measured and computed wall deflections of SID-1 yielded closely to the SID-2 wall deflections and indicates the buttress wall which was near SID-1 has no effect in reducing the wall deflection. According to Lim et al (2016) and Hsieh et al (2016), the wall deflection control mechanism of the buttress wall came from the frictional resistance buttress walls and adjacent soils due to the lateral wall deflection. Since the wall deflection at SID-1 was relatively small, due to the cross wall effect, then it could not effectively mobilize the shear resistance between the buttress wall and adjacent soils. Thus, in Case 1, it could well understand that the effect of the BW-A was very minor. Although the BW-A has a minor effect in reducing wall deflections, the contractor still constructed those BW-A for convincing the neighborhood that their buildings are completely safe. Hence, it was decided that the bottom of the BW-A was only founded at GL -14.9 m (3 m below the final excavation level) to cut the construction cost. Case 1 is a good example for showing the art of a decision making in the construction practice.

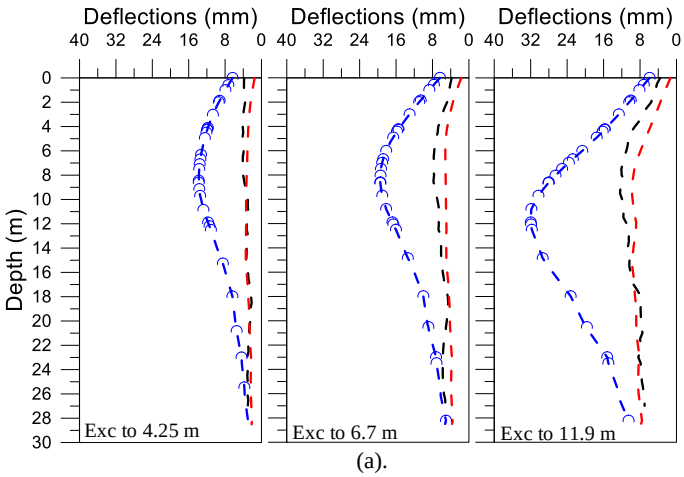

(a).

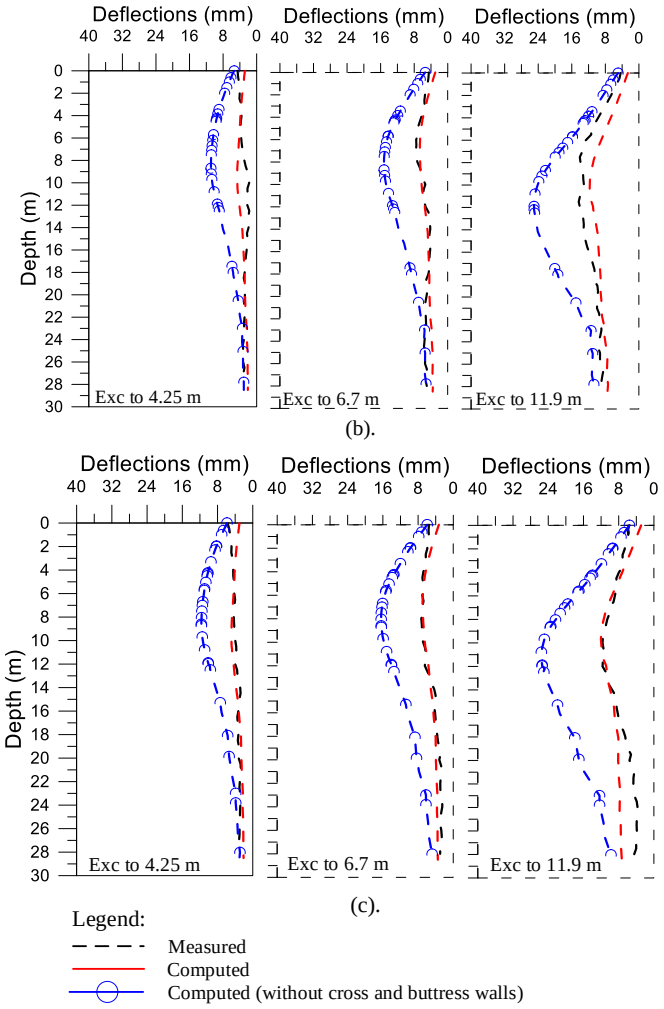

Figure 5 Comparison of lateral wall deflections from field measurement and those from the analysis for Case 1 (a) SID 1, (b) SID 2, and (c) SID 4

4. CASE STUDY 2

4.1 Project overview of Case 2

Case 2 is a new well-documented Case history which was located in Taipei, Taiwan. The building is a 32-stories building with eight levels of basement. Figure 6 shows the layout of the excavation along with the location of adjacent existing metro twin tunnel. The existing twin metro tunnel is active and located 14.5 m adjacent to the north diaphragm wall. According to the rapid metro system regulation, the allowable tunnel deformation induced by any surrounding constructions is 10 mm. Thus, Case 2 adopted 4 cross walls to meet the deformation criteria. The spacing of cross walls is 9.1 m and both ends of the cross walls were connected to the south and north diaphragm walls. Two buttress walls were also constructed at the east diaphragm wall to protect the adjacent gas station. In the simulation, the gas station was not modeled because it is considered insignificant. In Case 2, the main concern is to control the deformations of the adjacent twin metro tunnels induced by excavation which was located on the north side. The cross walls and the buttress walls design from GL -5 m to GL -53 m.

During the concreting of the diagram wall, a problem occurred. The weather was heavy rain during concreting the diaphragm wall panel on the north side, and causing debris and excavated silty sand soil which was deposited near the excavation trench flushed back into the trench together with rainwater run-off. The construction area became flooded and causing some debris and excavated silty sand soil which was deposited near the excavation trench flushed back into the trench. Thus, the toe of a diaphragm wall panel was misplaced, as shown in Figure 7. The toe of the defect diaphragm wall panel was at GL -33.3 m, while it was supposed to be at GL -53 m. The width of this defect panel is 6 m and located at the north diaphragm wall where existing twin metro tunnels were located 14.5 m away. Thus, the contractor stopped the project for a while and made some analyses and plans to convince that the existing twin metro tunnels are safe. Indeed, some auxiliary measures were proposed, such as the soil grouting and construct soldier piles to cover the defected panel. However, those plans were not discussed here because later it was concluded that those measures were not necessarily executed.

4.2 Subsurface soil profile and soil parameters of Case 2

Figure 8 shows the profile of the excavation and the subsurface soil conditions along with their physical properties and strength parameters. The groundwater level was located at GL -3.0 m. The excavation depth was 28.8 m, which was completed in nine stages using the top-down construction method and the modeling stages. In brief, each level of concrete floor slabs was installed directly after an excavation stage. The dewatering was performed inside the excavation zone and was planned to meet the safety against upheaval failure. Table 5 and Table 6 list the walls, slabs and struts parameters used for analysis, respectively. Furthermore, Table 7 lists the soil parameters used for analysis. All of the parameters in the tables were evaluated according to the methods discussed in the preceding section.

Table 5 The walls and slabs input parameters for Case 2

Type	Model	t (m)	f_c' (MPa)	E (kPa)
Diaphragm wall		1.2		
Basement slabs (1F, B1F ,B2F)		0.15	27.45	24624591
Basement slabs (B3F-B7F)		0.45		
Basement slabs (B8F)	Plate	0.2		
Buttress and cross walls-up		0.6	10.3	15083998
Buttress and cross walls-down		0.6	27.45	24624591
Tunnel Lining		0.25	27.45	24624591

Table 6 The struts input parameters for Case 2

Strut	Model	A (m^2)	E (GPa)
2Hx400x400x13x21	Node-to-node anchor	0.0437	210

4.3 Analysis result and discussion of Case 2

Figure 9 shows the plan view of computed results. Obviously, for the Case without cross walls and buttress walls, the existing twin tunnels were deformed and the deformed length was around 105 m where the maximum value was located toward the excavation area. Meanwhile, when the cross walls and the buttress walls were installed, the deformation of the twin tunnels was negligible.

Moreover, Figure 10 shows the computed diaphragm wall deflection and the tunnel deformations meshes. The without cross walls and buttress walls and the using cross walls and buttress walls cases are illustrated in Figures 10(a) and 10(b), respectively. The maximum tunnel deformation induced by excavation was 31 mm, where no cross walls and buttress walls were applied The tunnel-A tends to move toward the excavation area diagonally. Meanwhile, when cross walls and buttress walls were constructed, it was reduced to 4.7 mm and meet the deformation criteria, although the diaphragm wall defected. Although the measured data were not presented here due to Case sensitive, the computed results were believed could demonstrate the actual situation because the numerical analysis is one of the effective ways to study complex soil-structure interaction problem (Huang et al., 2013), hence the

computed results are believed could well capture the actual situation. According to the performed analysis, additional auxiliary measures besides cross and buttress walls, such as cement grouting or soldier piles, were not necessarily required. The cross walls and buttress walls were sufficient to control the tunnels deformations induced by deep excavation. The reason was due to the spacing of cross walls was dense and yielded the stiffness of the retaining wall system became very rigid and the wall deflections became very small. Hsieh et al., 2013 also concluded that the smaller the cross wall spacing, the larger the effect of the cross wall in reducing the lateral wall deflection was. Furthermore, Case 2 is a good example of using a dense interval of cross walls in protecting adjacent infrastructures.

5. CONCLUSIONS

Based on the three-dimensional finite element analyses results of two excavation Cases with cross walls and buttress walls, it was found that cross walls were very effective in reducing the lateral wall deflection. As a consequence, deformation of adjacent properties induced by excavation could be well controlled.

According to Case 1, the maximum lateral deflections at the SID-1 and SID-2 were reduced 57%, compared to no cross walls and buttress walls installation. When the lateral wall deflection had been reduced to a very small value, the application of buttress walls was insignificant because the relative movement between the buttress wall and adjacent soil was very small which causing the frictional resistance between the buttress wall and adjacent soil was not effectively mobilized.

Based on Case 2, the dense interval between cross walls yielded a very rigid retaining wall system. As a consequence, although the diaphragm wall defected at a certain location, the tunnels deformation induced by excavation still in the tolerable value, that was 4.7 mm. Hence, extra auxiliary measures such as soil grouting or soldier piles were not necessarily adopted to tackle the problem of the defect diaphragm wall.

6. ACKNOWLEDGMENT

The authors acknowledge the support provided by the Ministry of Science and Technology in Taiwan via grant number MOST103-2221-E-011-070-MY3. The authors would like to thank Sino Geotechnology, Inc. and Soonwell, Inc for the provision of detailed geotechnical information on the case studies.

Table 7 Soil input parameters for Case 2

Soil layer	Depth (m)	Description	Drainage type	γ_t (kN/m^3)	OCR	K_0	ϕ' (deg)	c' (kPa)	E_{50}^{ref} (kPa)	E_{oed}^{ref} (kPa)	E_{ur}^{ref} (kPa)	m
1	0 - 5.2	SF/ML1	Undrained	18.4	4.5	1.07	28	0	7457	5220	22370	1
2	5.2 - 9.5	SM1	Drained	19.3	1.6	0.61	31	0	10507	15761	31522	0.5
3	9.5 - 14.6	CL1	Undrained	18.9	1.5	0.61	30	0	8961	6273	26883	1
4	14.6 - 17.4	SM2	Drained	19.4	1.2	0.53	31	0	16609	24913	49826	0.5
5	17.4 - 25.5	ML2	Undrained	19.6	1.1	0.59	26	0	11585	8110	34756	1
6	25.5 - 28.8	SM3	Drained	19.6	1.1	0.51	31	0	18319	27478	54956	0.5
7	28.8-31.4	CL2	Undrained	19.8	1.1	0.51	31	0	12234	8564	36701	1
8	31.4 - 48.2	SM4	Drained	19.6	1.1	0.51	31	0	19438	29158	58315	0.5
9	48.2 - 55	CL/ML	Undrained	20.1	1.1	0.46	34	0	13706	9594	41117	1
10	55 - 80	Gravel	Drained	19.6	1.1	0.40	38	0	85000	85000	255000	0.5

Note: p^{ref} = 100kPa and υ_{ur} = 0.2 for all types of soils

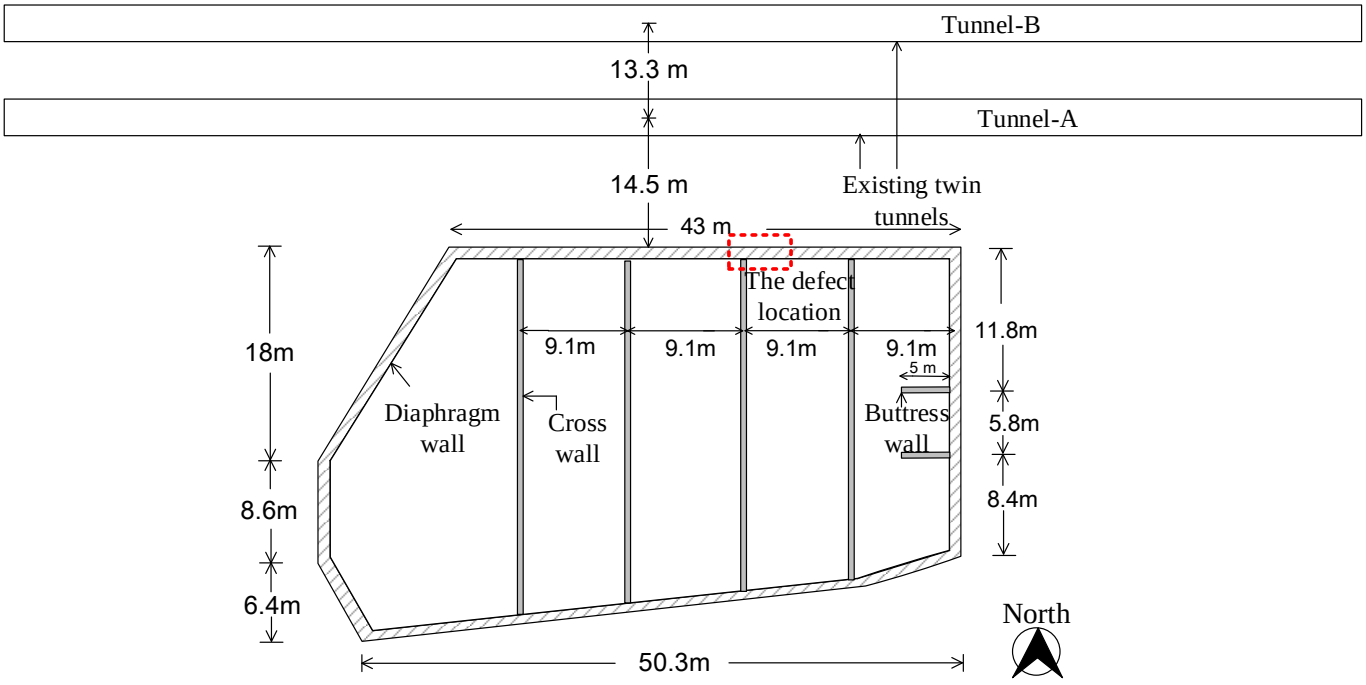

Figure 6 The geometry of excavation for Case 2

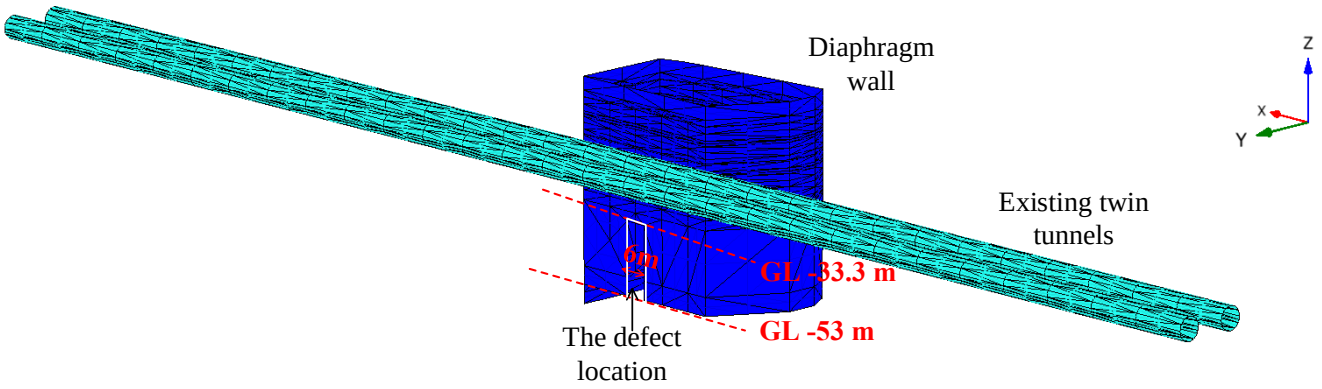

Figure 7 Three-dimensional finite element mesh of the diaphragm wall and existing twin tunnels

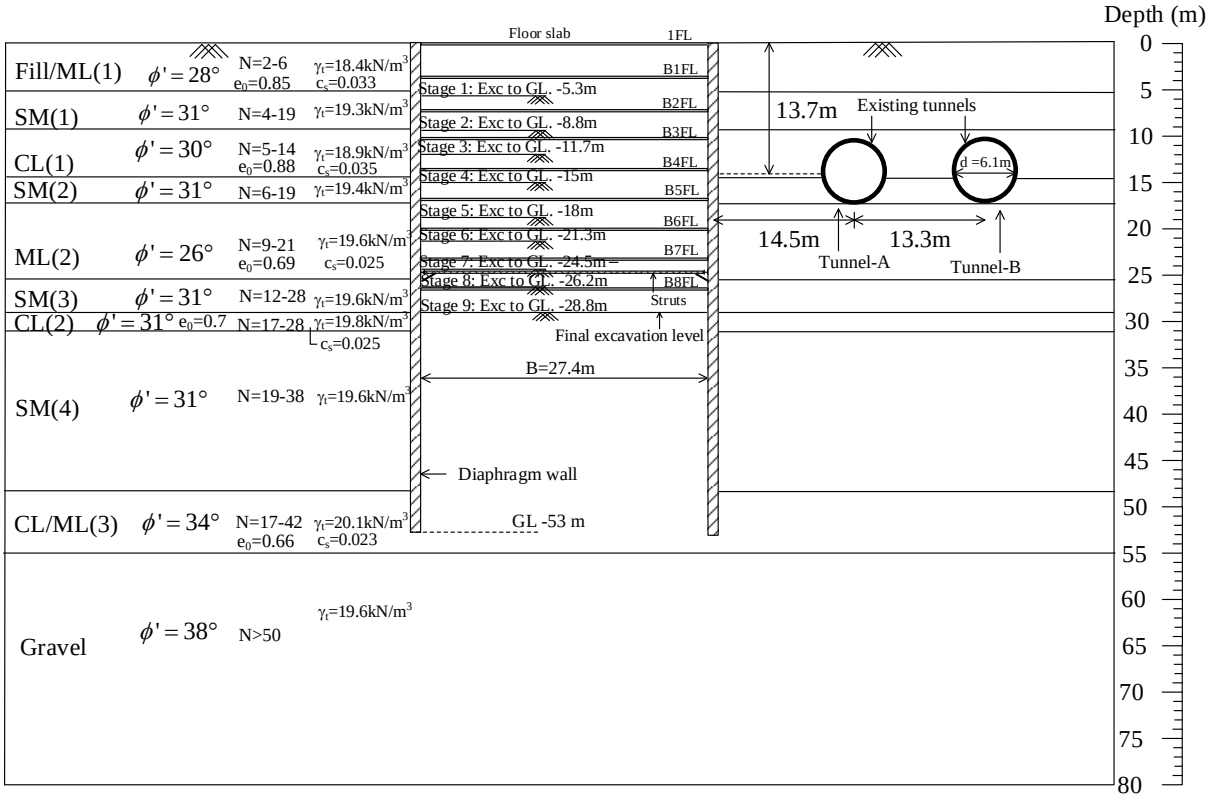

Figure 8 Profile of the excavation sequence and subsurface soil layers for Case 2

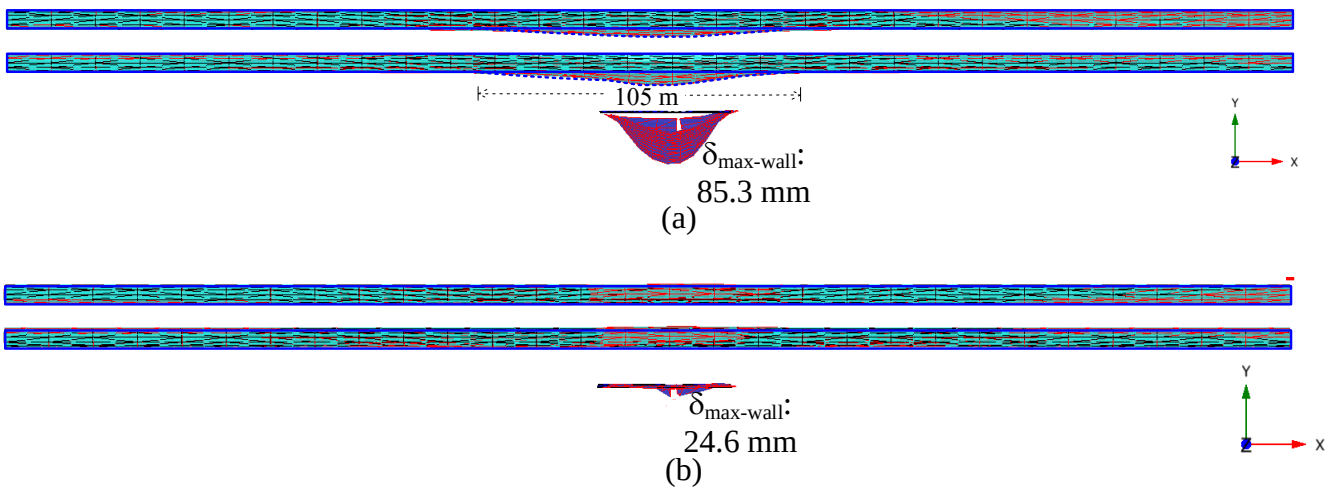

Figure 9 Plan view of the north diaphragm wall and the twin tunnels deform mesh (a). Without cross walls and buttress walls, (b). With the cross walls and the buttress walls

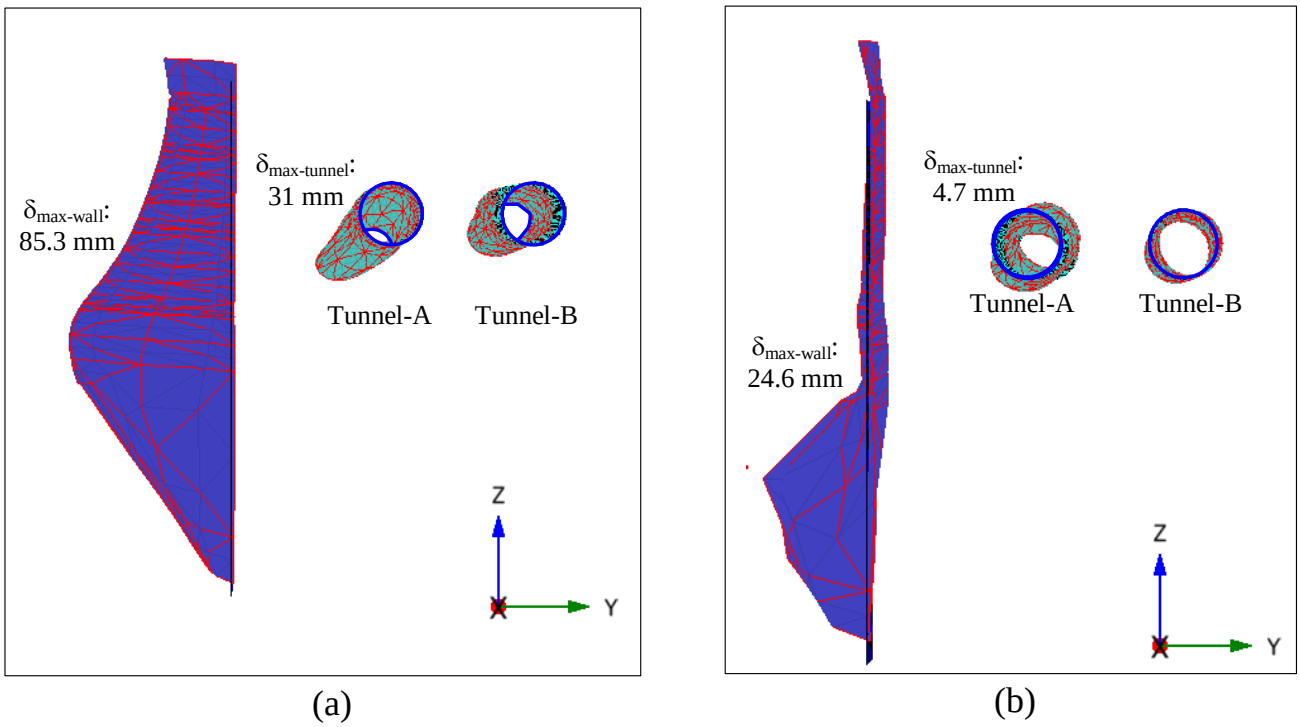

Figure 10 The computed deformed mesh of the north diaphragm wall and the twin tunnels (a). Without cross walls and buttress walls, (b). With the cross walls and the buttress walls

7. REFERENCES

ACI Committee 318. (1995) Building code requirements for structural concrete and commentary; ACI 318R-American Concrete Institute (ACI), Farmington Hills.

Brinkgreve, R. B. J., Engin, E., and Swolfs, W. M. (2013) PLAXIS 3D Manual; Delft, Netherlands, PLAXIS.

Calvello, M., and Finno, R. (2004) "Selecting parameters to optimize in model calibration by inverse analysis". Computer and Geotechnics, 31(5), pp. 410-424.

Comodromos, E. M., Papadopoulou, M. C., and Konstantinidis, G. K. (2013) "Effects from diaphragm wall installation to surrounding soil and adjacent buildings". Computer and Geotechnics, 53, pp. 106–121.

Dong, Y. P., Burd, H. J., and Houlsby, G. T. (2016) "Finite-element analysis of a deep excavation Case history". Geotechnique, 66(1), pp. 1–15.

Elshafie, M. Z., Choy, C., and Mair, R. J. (2013). "Centrifuge modeling of deep excavations and their interaction with adjacent buildings". Geotechnical Testing Journal, 36 https://doi.org/10.1520/GTJ20120209

Huang, X., Schweiger, H. F., and Huang, H. (2013) "Influence of Deep Excavations on Nearby Existing Tunnels". International of Geomechanics, 13(2), pp. 170-180.

Hsieh, P. G., Ou, C. Y., and Lin, Y. L. (2013) "Three-dimensional numerical analysis of deep excavation with cross walls". Acta Geotechnica, 8, pp. 33-48.

Hsieh, P. G., Ou, C. Y., Lin, Y. K., and Lu, F. C. (2015) "Lesson learned in design of an excavation with the installation of buttress walls". Journal of GeoEngineering, 10(2), pp. 63-73.

Hsieh, P. G., Ou, C. Y., and Hsieh, W. H. (2016) "Efficiency of excavations with buttress walls in reducing the deflection of the diaphragm wall". Acta Geotechnica, DOI 10.1007/s11440-015-0416-6.

Hwang, R. N., and Moh, Z. C. (2008) "Evaluating effectiveness of buttresses and cross walls by reference envelopes". Journal of GeoEngineering, 3(1), pp. 1-11.

Jaky, J. (1944) "The coefficient of earth pressure at rest". Journal for Society of Hungarian Architects and Engineers, 78(22), pp. 355–358 (In Hungarian).

Khoiri, M., and Ou, C. Y. (2013) "Evaluation of deformation parameter for deep excavation in sand through Case histories". Computers and Geotechnics, 47(1), pp. 57-67.

Ladd, C. C., Foott, R., Ishihara, K., Schlosser, F., and Poulos, H. G. (1977) "Stress-deformation and strength characteristics". Proceedings of the 9th international conference on soil mechanics and foundation engineering, 2, pp. 421–494: Tokyo.

Lim, A., Ou, C. Y., and Hsieh P. G. (2010) "Evaluation of clay constitutive models for analysis of deep excavation under undrained conditions". Journal of GeoEngineering, 5(1), pp. 9-20.

Lim, A., Hsieh, P. G., and Ou, C. Y. (2016) "Evaluation of buttress wall shapes to limit movements induced by deep excavation". Computer and Geotechnics, 78, pp. 155-170.

Lim, A., and Ou C. Y. (2017) "Stress paths in deep excavations under undrained conditions and its influence on deformation analysis." Journal of Tunneling and Underground Space Technology, 63, pp. 118-132.

Ou, C. Y. (2016) "Finite element analysis of deep excavation problems". Journal of GeoEngineering, 11(1), pp. 91-101.

Ou, C. Y., Teng, F. C, Seed, R. B., and Wang, I. W. (2008) "Using buttress walls to reduce excavation-induced movements". Proceedings of the Institution of Civil Engineers Geotechnical Engineering, 161(GE4), pp. 209–222.

Ou, C. Y., Lin, Y. L., and Hsieh, P. G. (2006) "A Case record of an excavation with cross walls and buttress walls". Journal of GeoEngineering, 1(2), pp. 579–86.

Ou, C. Y., Hsieh, P. G., and Lin, Y. L. (2011) "Performance of Excavations with cross walls". Journal of Geotechnical and Geoenvironmental Engineering, 137(1), pp. 94-104.

Schanz, T., Vermeer, P. A., and Bonnier, P. G. (1999) "Formulation and verification of the Hardening-Soil model". Beyond 2000 in Computational Geotechnics. Brinkgreve ed, Rotterdam Balkema, pp. 281-290.